

# COMSOL SIMULATIONS OF MAGNETIC FLUX GENERATED BY PERMANENT MAGNETS WITH RING GEOMETRIES

ASMA SAMOH<sup>1</sup>, NUANJUTA NIAMJAN<sup>1</sup>, CHAIROTE YAIPRASERT<sup>1</sup>,  
YAOWARAT SIRISATHITKUL<sup>2</sup>, CHITNARONG SIRISATHITKUL<sup>1\*</sup>

*Manuscript received: 11.05.2019; Accepted paper: 22.07.2019;*

*Published online: 30.09.2019.*

**Abstract.** *Magnetic flux generated by neodymium-iron-boron magnets of three different configurations are calculated and compared by using COMSOL Multiphysics simulation. For a magnetic ring, the substantial flux density of 0.6-0.7 T is obtained in the bore and the edge. The values are increased beyond 1 T in the gap between inner and outer concentric rings in the second structure. The magnetic flux density is fairly uniform in the circumferential direction. Finally, moderate fields around 0.6 T in spaces between magnetic bars arranged into concentric arrays can be utilized. In this structure, the magnetic flux density along the radial direction measured from the center of the ring peaks at two distances corresponding to two arrays of magnets. These different profiles of magnetic field can be implemented in devices and experiments of different requirements.*

**Keywords:** *Permanent magnet, Hollow cylinder, Magnetic flux density, COMSOL Multiphysics.*

## 1. INTRODUCTION

Magnetic fields from permanent magnetic rings and hollow cylinders are utilized in numerous devices including magnetic separators, magnetic bearing, holding devices, actuators and generators. In addition, the influence of magnetic field on biological systems referred to as magnetobiology is receiving much attention [1]. It is necessary to design structures supplying magnetic flux densities in which specimens are subjected to. Uniform and substantial magnetic fields in the bore are desirable in most cases but different profiles may also be needed in some circumstances such as magnetic refrigerators. It is therefore a topic of interest to analyse and simulate the magnetic flux distribution from magnets with different ring and cylindrical geometries by using analytical and numerical methods. Magnetic fields generated by hollow cylindrical magnets were calculated analytically by Reich et al. [2]. Bjørk compared hollow cylinders with varying magnetization directions [3] and the effects of demagnetising field in such structure were shown by Beleggia et al. [4]. For magnetic rings, magnetic fields were analysed by Babic et al. [5] and Ravaud et al. [6]. In additions, different geometries were investigated including nanostructured cylinders by Suarez et al. [7] and arrays of magnets by Vokoun et al. [8].

---

<sup>1</sup> Walailak University, School of Science, 80160 Nakhon Si Thammarat, Thailand.

E-mail: [iama62@gmail.com](mailto:iama62@gmail.com); [juzzzz5@gmail.com](mailto:juzzzz5@gmail.com); [ychairot@mail.wu.ac.th](mailto:ychairot@mail.wu.ac.th);

**Corresponding author:** [chitnarong.siri@gmail.com](mailto:chitnarong.siri@gmail.com).

<sup>2</sup> Walailak University, School of Informatics, 80160 Nakhon Si Thammarat, Thailand.

E-mail: [kinsywu@gmail.com](mailto:kinsywu@gmail.com).

This research investigates the magnetic flux generated by three geometries of permanent magnets, namely a ring, a concentric ring and concentric arrays. Numerical calculations are carried out by COMSOL Multiphysics [9]. The software was recently used in calculations of magnetic fields in a variety of devices such as magnetic refrigerators [10], maglev [11] and actuators [12].

## 2. SIMULATION PROCEDURE

Three geometries of permanent magnets are investigated. With neodymium-iron-boron (Nd-Fe-B) as the material, the remanent flux density is set as 1.3 T. For the first structure, the magnetic ring is 20 mm in inner radius, 80 mm in outer radius and 23 mm in height as shown in Fig. 1. The next structure in Fig. 2 is concentric hollow cylinders of 23 mm in height. The internal ring is 20 mm in inner radius and 50 mm in outer radius, whereas the external ring is 50 mm in inner radius and 80 mm in outer radius. Finally, the third geometry is composed of 26 permanent magnetic bars of  $25 \times 25 \times 23$  mm<sup>3</sup> in size. Eighteen bars are arranged into an circular array of 145 mm in radius and an inner circular array composed 8 bars is 55 mm in radius. Both arrays share the same center as shown in Fig. 3. The remanent magnetic flux density ( $\mathbf{B}_r$ ) is set in the Z-axis. For the concentric structures in Fig. 2 and Fig. 3,  $\mathbf{B}_r$  of the internal and external parts are in the opposite directions.

Numerical simulations were carried out by finite element method using COMSOL Multiphysics version 5.3 program. Free triangular elements were implemented in 2D axisymmetric for a half of model. The magnetic flux density ( $\mathbf{B}$ ) generated by the permanent magnetic ring was derived from the magnetic vector potential ( $\mathbf{A}$ ).

$$\mathbf{B} = \nabla \times \mathbf{A} \quad (1)$$

$\mathbf{A}$  is obtained from the integral of the current density ( $\mathbf{J}$ ) over the position.

$$\mathbf{A} = \frac{\mu_0}{4\pi} \int \frac{\mathbf{J}(\mathbf{r}')}{|\mathbf{r} - \mathbf{r}'|} \tau d \quad (2)$$

where  $\mu_0$  is magnetic permeability in vacuum.  $\mathbf{r}'$  and  $\mathbf{r}$  are positional vectors.

The magnetic flux density in any medium is;

$$\mathbf{B} = \mu_0 \mu_r \mathbf{H} \quad (3)$$

where  $\mu_r$  is relative magnetic permeability and  $\mathbf{H}$  is magnetic field strength.

For ferromagnetic materials, the magnetic flux density is also dependent on  $\mathbf{B}_r$ .

$$\mathbf{B} = \mu_0 \mu_r \mathbf{H} + \mathbf{B}_r \quad (4)$$

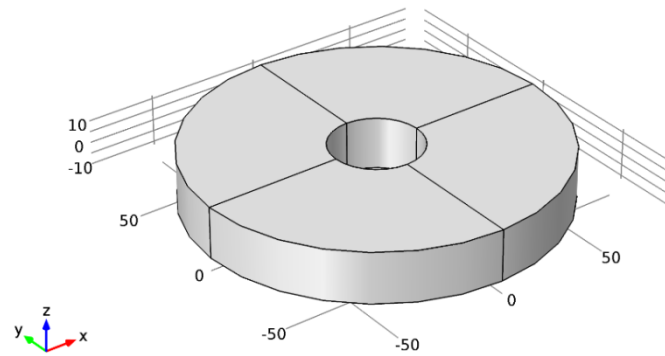


**Figure 1. Geometry of the permanent magnetic ring.**

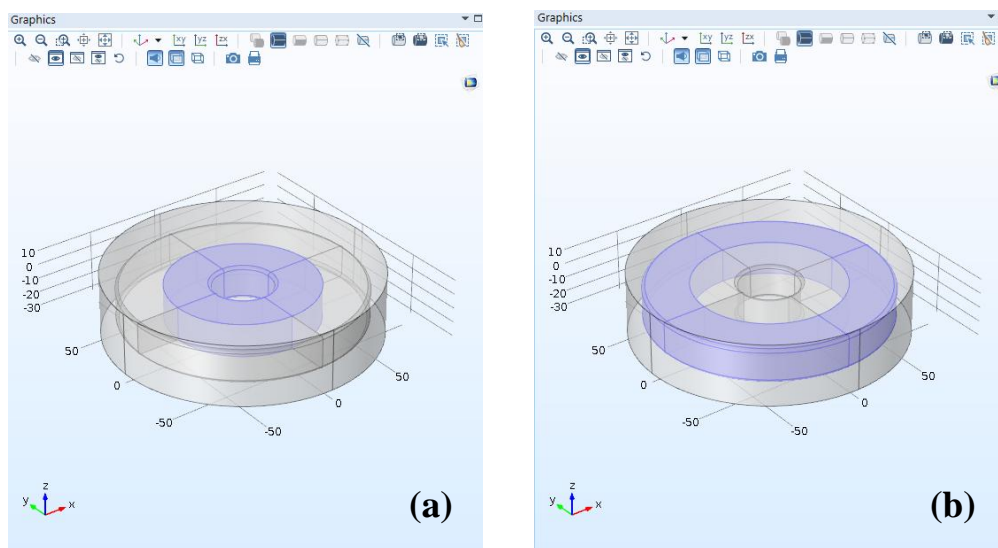


**Figure 2. Geometry of the concentric hollow cylinders; (a) the highlighted internal ring and (b) the highlighted external ring.**

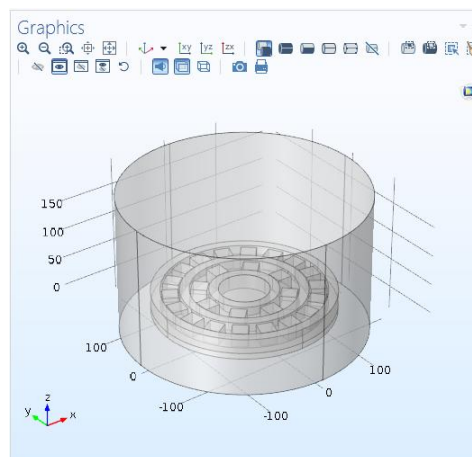


**Figure 3. Geometry of array of magnets arranged into concentric rings.**

### 3. SIMULATION RESULTS AND DISCUSSION

#### 3.1. PERMANENT MAGNETIC RING

In Fig. 4, profiles of magnetic flux in two cross-sectional planes are displayed by COMSOL ranging from the highest density in red color to the lowest in blue color. Because of the cylindrical geometry, the distribution are symmetric in both planes and the magnetic flux is concentrated at the inner and outer edges. The magnetic flux density is plotted as a function of the distance from the center of the ring in Fig. 5. Two peaks are located around the inner and outer radii of the ring. It follows that the substantial magnetic field can be utilized in the bore and around the ring with the decrease in magnitude away from the structure. The contour of flux lines in a segment of the ring illustrated by SUPERFISH and the COMSOL simulations are compared in Fig. 6. The two-dimensional simulations by both programs are in good agreements and consistent with the published analysis [5,6]. In this configuration, magnetic flux is depleted inside and directed towards inner and outer edges of the magnetic ring.

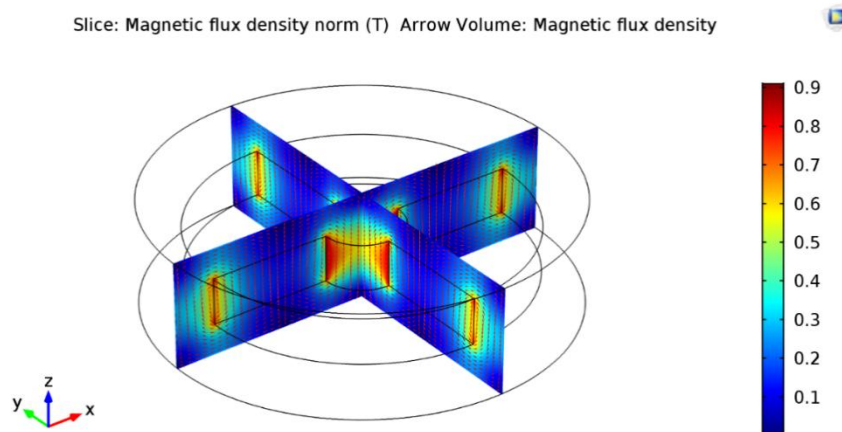


Figure 4. Profiles of magnetic flux density generated by a permanent magnetic ring.

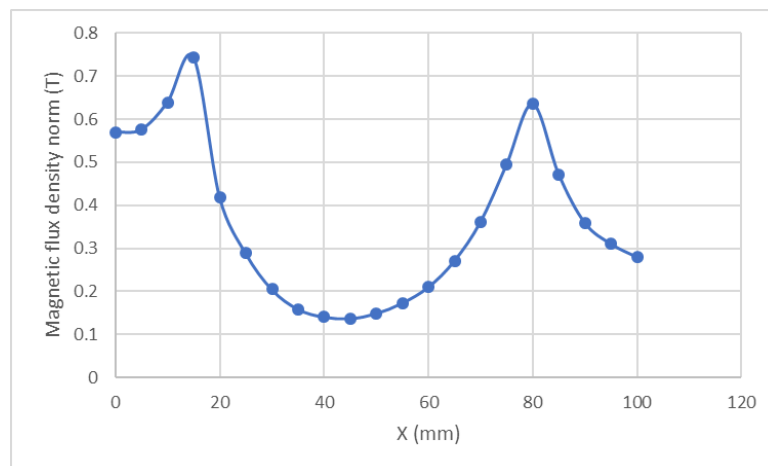
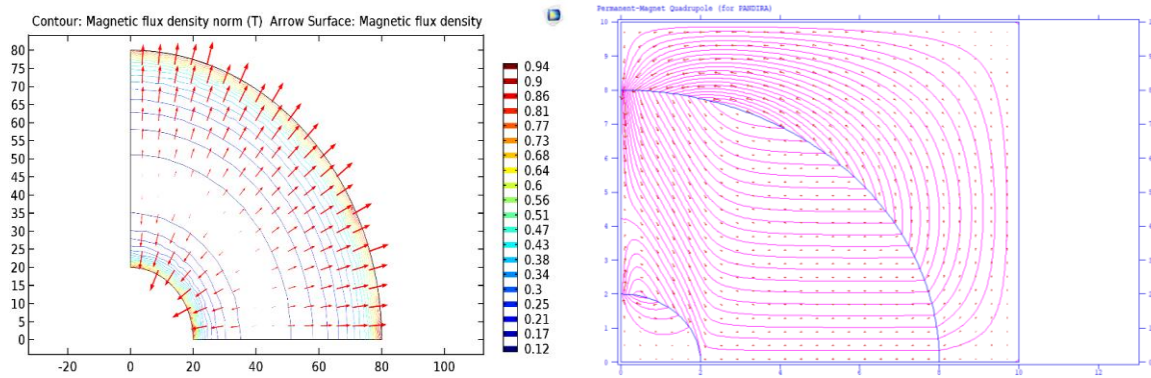


Figure 5. Radial variations of magnetic flux density generated by a permanent magnetic ring.



**Figure 6. Magnetic flux contours simulated COMSOL Multiphysics 5.3 and Poisson SUPERFISH 7.0.**

### 3.2. CONCENTRIC PERMANENT MAGNETIC RINGS

For the concentric hollow cylinders, profiles of magnetic flux in Fig. 7 drastically differ from those generated by the single magnet in Fig. 4. The distribution remains symmetric in the cross-sectional plane but the flux is largely concentrated at the boundary between two rings. The flux densities at the inner and outer edges are reduced to 0.8 T. It is noted that a large flux density as high as 1.2 T is obtained at the expense of that in the bore. The flux leakage outside the magnetic assembly is thus reduced by such configurations.

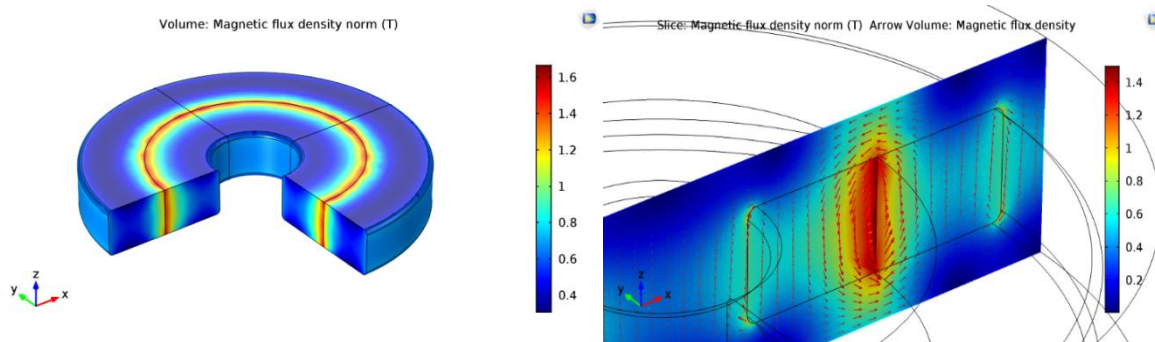


**Figure 7. Profiles of magnetic flux density generated by concentric permanent magnetic ring.**

The magnetic flux density is plotted as a function of distance from the center in Fig. 8. In contrast to the single magnetic ring, the magnetic flux density is at the minimum in the bore and becomes fairly constant around 0.4 T inside the inner ring. The plot then suddenly rises as the increasing distance approaches the edge of the inner ring. The magnetic flux density is maximum at the gap between the inner and outer rings, consistent with the flux distribution shown in Fig. 7. At further distances inside the outer ring, the magnetic flux density reduces and then rises as the edge of the outer is reached. Fig. 8 also shows the effect of the gap between the inner and outer rings. With 7 varying gap sizes from 0 to 3 mm, the magnetic flux has reducing magnitudes while exhibits the same variation with distance from the center.

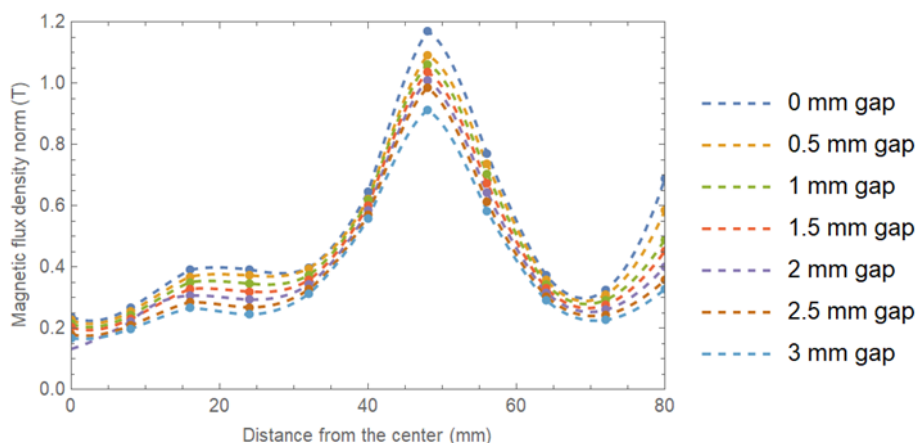


**Figure 8. Radial variations of magnetic flux density generated by a concentric permanent magnetic ring.**

The reduction in the magnetic flux density with enhancing gap between the inner and outer rings is also demonstrated in Fig. 9, ranging from 0.7 T to 0.3 T in the case of the largest gap of 3 mm. With exceptions for a few points in the case of 0 and 0.5 mm gap, the magnetic flux density is fairly uniform along the angular direction up to 80°.

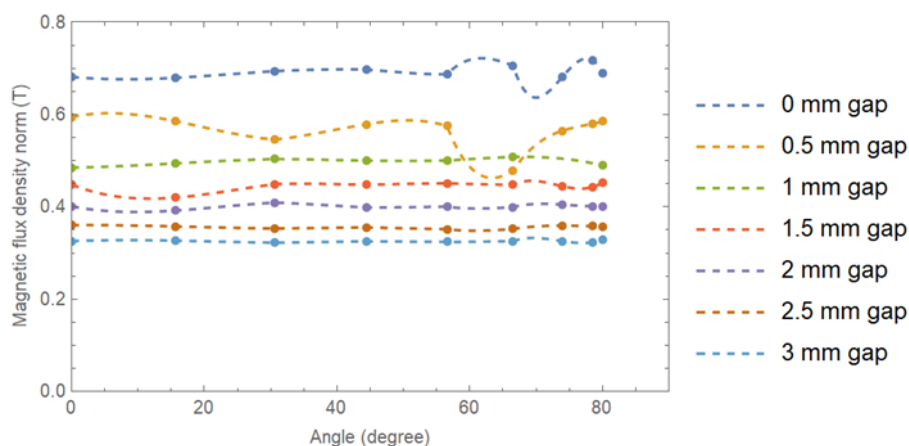


**Figure 9. Angular variations of magnetic flux density generated by a concentric permanent magnetic ring.**

### 3.3. CONCENTRIC PERMANENT MAGNETIC ARRAYS

In Fig. 10, profiles of magnetic flux generated by concentric arrays of permanent magnets drastically differ from those by the concentric magnetic rings in Fig. 7. The discrete structure results in a large decrease in the magnetic flux density. The dark blue areas in the center and between two arrays indicate the flux depletion. Instead, the magnetic flux concentrates between the magnetic bars forming into each ring. Red arrows pointing from the magnetic bars indicate the direction of magnetic flux lines. It follows that the moderate magnetic fields around 0.6 T can be utilized in 26 spaces between permanent magnetic bars.

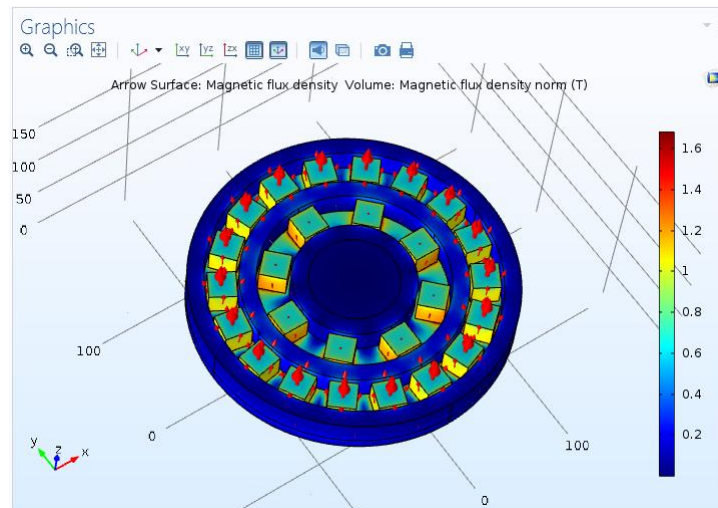


Figure 10. Profiles of magnetic flux density generated by concentric arrays of permanent magnets.

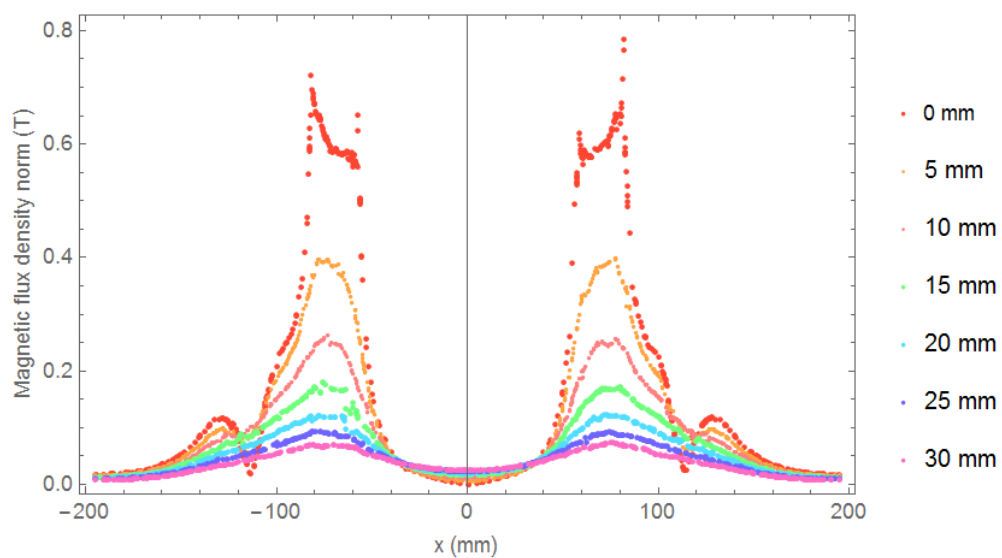


Figure 11. Radial variations of magnetic flux density generated by concentric arrays of permanent magnets at varying distances in the Z-axis up to 30 mm.

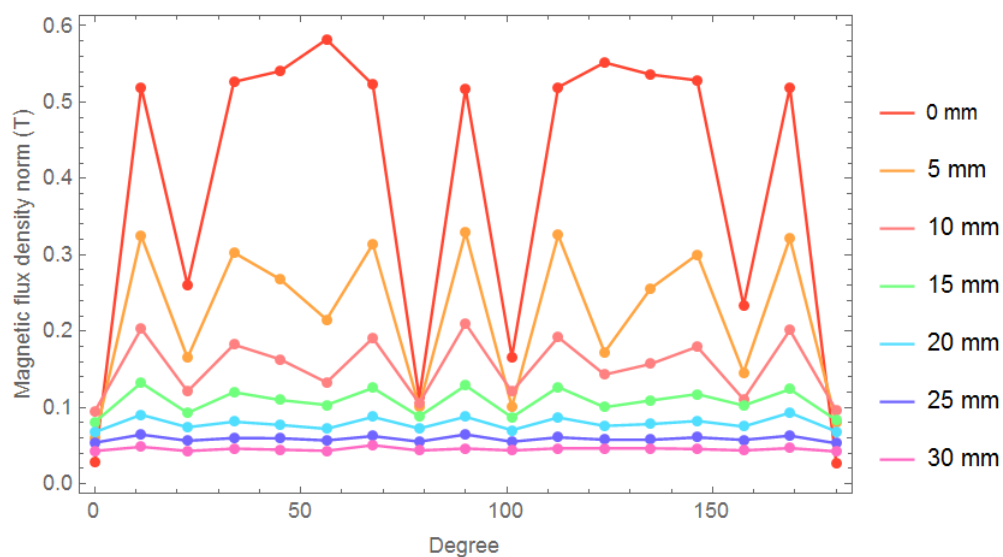


Figure 12. Angular variations of magnetic flux density generated by concentric arrays of permanent magnets at varying distances in the Z-axis up to 30 mm.

Fig. 11 shows a symmetric magnetic flux density as a function of distance from the center, and this fact is due to the symmetry in geometry. Similar to the concentric magnetic rings, the magnetic flux density is minimal in the center. The magnitude sharply enhances at the distance around the magnetic arrays, consistent with the flux distribution shown in Fig. 10. Furthermore, Fig. 11 and Fig. 12 compare the magnetic flux density away from the magnetic structure in the Z-axis. The variations are similar in all 7 different distances but the magnetic flux density is successively reduced with the increase in distances up to 30 mm. Unlike the concentric magnetic rings, the magnetic flux density as a function of angle in Fig. 12 is not uniform notably near the structure. Such clear luctuations in the case of 0-15 mm reflect the segmented magnetic structure.

#### 4. CONCLUSIONS

By selecting Nd-Fe-B as permanent magnetic materials with remanent flux density of 1.3 T, the numerical simulation by Comsol indicated the profiles of magnetic field generated by three different geometries of magnetic rings. Firstly, magnetic flux densities around 0.7 T were obtained in the bore of the ring whose inner and outer radii were 20 and 80 mm. The flux density was increased in the circumferential direction to over 1 T by placing two rings as a concentric structure. The utilizable space in the gap may be increased at the expense the maximum flux density. Finally, the magnetic field in the circumferential direction fluctuated in the case of separated permanent magnetic bars arranged into two concentric arrays. The plots of radial and angular variation of magnetic flux density were useful in designing devices and implementing in magnetobiology.

**Acknowledgements:** *The work is a part of Innovation Physics for Magnetic Cooling Industry program funded by Thailand Center of Excellence in Physics. The scholarship from Development and Promotion of Science and Technology Talents Project (DPST) for the first author is acknowledged.*

#### REFERENCES

- [1] Torres, J. et al., *J. Magn. Magn. Mater.*, **449**, 366, 2018.
- [2] Reich, F.A. et al., *Continuum Mech. Therm.*, **28**, 1435, 2016.
- [3] Bjørk, R., *J. Magn. Magn. Mater.*, **416**, 321, 2016.
- [4] Beleggia, M. et al., *J. Magn. Magn. Mater.*, **321**, 1306, 2009.
- [5] Babic, S. I., Akyel, C. *Prog. Electromagn. Res. C*, **5**, 71, 2008.
- [6] Ravaud, R. et al., *IEEE Trans. Magn.*, **44**, 1982, 2008.
- [7] Suarez, O.J. et al., *J. Magn. Magn. Mater.*, **324**, 1698, 2012.
- [8] Vokoun, D., Beleggia, M., *J. Magn. Magn. Mater.*, **350**, 174, 2014.
- [9] COMSOL AB, *Tegn ́ergatan 23, SE-111 40 Stockholm, Sweden.*
- [10] You, Y.H. et al., *J. Magn. Magn. Mater.*, **405**, 231, 2016.
- [11] Zheng, J. et al., *IEEE Trans. Appl. Supercond.*, **28**, 3600808, 2018.
- [12] Dragomir, F. et al., *J. Sci. Arts*, **2**(43), 523, 2018.
- [13] Halbach, K., Holsinger, R.F. *Part. Accel.*, **7**, 213, 1976.